Water Resources Management
https://doi.org/10.1007/s11269-025-04206-6

Evaluating the Impact of the Spatial Resolution of Digital Elevation Models on Flood Modelling

Ekundayo Abayomi Adesina[1] · **Joseph Olayemi Odumosu**[2] · **Oluibukun Gbenga Ajayi**[3] · **Ahmed Musa**[1] · **Ifeanyi Chukwudi Onuigbo**[1] · **Adeolu Richard Adesiji**[4]

Received: 3 February 2025 / Accepted: 31 March 2025

Abstract
Accurate flood modelling is crucial for effective disaster management. This study investigated the impact of different Digital Elevation Model (DEM) resolutions (1 m UAV, 10 m InSAR, and 30 m SRTM) on flood modelling within the Shiroro floodplain, Nigeria. Using the Shallow Water Equations (SWE) implemented in MATLAB to assess flood levels along 12 river channels within the study area, the findings demonstrated that the UAV-derived 1 m DEM provided the most accurate flood predictions, exhibiting lower RMSE values (0.249 m) compared to InSAR (0.352 m) and SRTM (0.455 m). The higher resolution of the UAV DEM captured topographic details more effectively, leading to more accurate flood predictions, in contrast to the low resolution of InSAR and SRTM, which resulted in an overestimation of flood risk due to the smoothing and generalization of topographic features. These results highlight the critical importance of using high-resolution DEMs, particularly those derived from UAV imagery, for accurate flood modelling and effective flood risk management, as these high-resolution datasets can significantly improve flood forecasting, refine flood hazard maps, and inform targeted flood mitigation measures, ultimately enhancing disaster preparedness and response within the Shiroro floodplain and beyond.

Keywords DEM Resolution · Flood Modelling · Flood Risk Management · InSAR DEM · Shiroro Floodplain · UAV DEM

✉ Ekundayo Abayomi Adesina
adesinageoworldsolutions@gmail.com

[1] Department of Surveying and Geoinformatics, School of Environmental Technology, Federal University of Technology, Minna, Nigeria

[2] Faculty of Environmental Science, Department of Geomatics, University of Benin, Benin City, Nigeria

[3] Faculty of Engineering and the Built Environment, Department of Land and Spatial Sciences, Namibia University of Science and Technology, Windhoek, Namibia

[4] Department of Civil Engineering, School of Engineering Technology, Federal University of Technology, Minna, Nigeria

Published online: 23 April 2025

1 Introduction

Flooding is a significant global challenge, causing substantial economic and social disruption worldwide (Sridhar et al. 2019; Moustakis et al. 2021). As climate change intensifies, the frequency and severity of flood events increase, necessitating robust and accurate flood prediction and mitigation strategies (Sridhar et al. 2021). Hydrological and hydraulic models are essential for assessing flood risk, guiding decision-making, and facilitating effective flood management (Kemp and Daniell 2020). These models rely heavily on Digital Elevation Models (DEMs) to represent the terrain and drive the water flow simulation (Gu et al. 2019; Fang et al. 2020). However, the spatial resolution of DEMs significantly influences the accuracy and reliability of modelling outcomes (Pedrozo-Acuna et al. 2015; Savage et al. 2016; Ajayi 2023).

Hydrological models simulate the hydrologic cycle and predict flood events by analysing water flow within the river and stream systems (Dang et al. 2020). These models consider land use, topography, soil moisture, evaporation, and precipitation. They are crucial for flood modelling as they identify flow characteristics, provide data for hydraulic analysis, pinpoint high-risk flood areas, and inform emergency response planning and flood risk reduction strategies (Kim et al. 2020; Sahu et al. 2023). A variety of hydrological modelling approaches exist, including conceptual models (e.g., HBV, HYMOD), lumped rainfall-runoff models (e.g., GR4 J, SMAP, MGB-IPH), hybrid models, and distributed models (Jayanthi et al. 2022; Nageswara et al., 2022). However, limitations include simplification and approximation errors, parameter uncertainty, limited representation of hydrological processes, high computational requirements, and the need for extensive data and calibration.

Previous studies consistently demonstrate the significant impact of DEM resolution on hydrological modelling outcomes, with higher resolutions (e.g., 5–10 m) generally improving topographic representation, enhancing streamflow simulation accuracy, and improving flood-prone area identification compared to lower resolution DEMs (e.g., 30–1000 m) (Saksena and Merwade 2015; Talchabhadel et al. 2021). The optimal DEM resolution varies depending on the application, study area, and model requirements, with higher resolutions often necessary for detailed flood modelling studies and lower resolutions potentially sufficient for larger-scale hydrological assessments (Mukherjee et al. 2013; Talchabhadel et al. 2021). This impact has been extensively investigated, with studies focusing on the influence of DEM resolutions on watershed physical characteristics (Da Costa et al., 2019), enhanced streamflow simulations using varying resolutions (Massazza et al. 2019; Zhang et al. 2019), and the influence of different resolutions on SWAT model predictions for water availability (Utlu and Ozdemir, 2020). These studies, along with others (Cook and Merwade 2009; Coveney and Fotheringham 2011), collectively demonstrate the significant impact of DEM resolution on hydrological modelling outcomes, with higher resolutions generally leading to improved model performance and accuracy.

However, while previous studies have investigated the impact of DEM resolution on hydrological modelling in various contexts, such as those conducted in temperate climates and smaller catchments (Simpson et al. 2016; Schuman and Bates 2020), limited studies have specifically examined its influence within the unique topographic and hydrological characteristics of the Shiroro Dam watershed in Nigeria. This region, crucial for Nigeria's energy production and water supply, lacks adequate hydrological studies, and the influence of DEM resolution on modelling outcomes remains largely unknown. This study investigates the impact of DEM spatial resolution on hydrological and hydraulic modelling within the Shiroro Dam watershed. Specifically, it will evaluate the effect of DEM resolution on streamflow simulation, assess the impact of DEM resolution on water yield estimation, and compare the performance of different DEM resolutions to identify the optimal resolution for achieving the most accurate and reliable results within the study area. This study contributes to the existing literature by examining the influence of DEM resolution within a tropical environment, specifically the Shiroro Dam watershed in Nigeria, characterised by distinct hydrological regimes and complex topography. Furthermore, it provides valuable insights for improving flood risk assessment, informing early warning systems, and supporting sustainable water resource management in the Shiroro Dam watershed and other similar contexts.

2 Materials and Methods

2.1 Materials

The study used various data types to achieve its objectives, including secondary data from existing literature and primary data collected directly from the field. It also employed tools, software, and equipment to obtain and process this data. Table 1 provides detailed information on the specific data sources and the resources utilised in this study. Figure 1 presents the methodological workflow of the study.

2.2 Study Area

Shiroro Dam floodplain, which is in the Shiroro Local Government Area of Niger State, Nigeria was used as the study area. It lies between Latitudes 09° 44’ 00” and 10° 11’ 30”N and longitudes 6° 27’ 00” to 7° 05’ 30”E and located 550.364 m downstream from where the Rivers Kaduna and Dinya converge, with the Shiroro hamlet being a significant point of attraction.

The Rivers Dinya, Sarkin Pawa, Guni, Erena, and Muyi are among the tributaries that make up the Shiroro basin, and all contribute to the flow of the River Kaduna. Northwest-to-southeast and north-to-south flow patterns are present in the drainage pattern, which efficiently drains the low-lying area with a few small hills scattered throughout. The study area’s land use is mostly a combination of agricultural and residential uses, which reflects the socioeconomic makeup of the study area. The Shiroro Dam, designed for hydroelectric power generation, significantly influences the hydrological dynamics of the studied area. The region’s notable elevation variations make it more vulnerable to flood damage, which puts infrastructure and nearby residents in serious danger.

A tropical monsoonal environment with distinct wet and dry seasons prevails in the research area. The rainy season lasts 162–200 days annually, beginning in April (Anzaku et al. 2019). According to Suleiman (2014), the average yearly temperature falls between 27 °C and 35 °C. The region frequently experiences flooding yearly, especially during the rainy season, with significant flooding occurrences recorded between 1990 and 2023 (NEMA, 2024). The alleged cause of these floods is the controlled water release through the dam flood control outlets, which reduces the amount of water and avoids possible dam failure

Table 1 Details of the materials data used for the study

Primary Data	Source	Instrument	Processing software	Spatial resolution	Data acquisition date	Accuracy
UAV-Derived DEM	Field mission	UAV Trimble UX5	Trimble Business Center Photogrammetry Module application (version 3.30)	1 m	2024	0.1 m
River channel bathymetry	Field mission	Dual-frequency GPS receiver and Hi-Target DH Light Echo Sounder	ArcGIS 10.4	-	2024	-
Secondary data	Source	Instrument	Processing software	Spatial resolution	Date of data acquisition	Accuracy
InSAR 10 m DEM	https://scihub.copernicus.eu/dhus/#/home.	N/A	Sentinel Applications Platform (SNAP) version 8.0	10 m	2022	1 m
SRTM 30 m DEM	http://earthexplorer.usgs.gov	N/A	ArcGIS 10.4	30 m	2022	3–4 m
Settlements flooded	NSEMA	N/A	N/A	-	2022	-
Settlement data for the study area	NIGIS	N/A	N/A	-	2022	-
Water level, rainfall, inflow, temperature, and outflow	Shiroro Dam Authority (hydrological data)	N/A	N/A	-	2020	-

(Usman and Ifabiyi 2012; Abayomi et al. 2015). Although this regulated discharge for dam safety, it may make flooding downstream worse.

An overview of the study area's geography and salient characteristics is presented in Figure 2. Understanding flood dynamics and how DEM resolution affects flood modelling accuracy requires this spatial context.

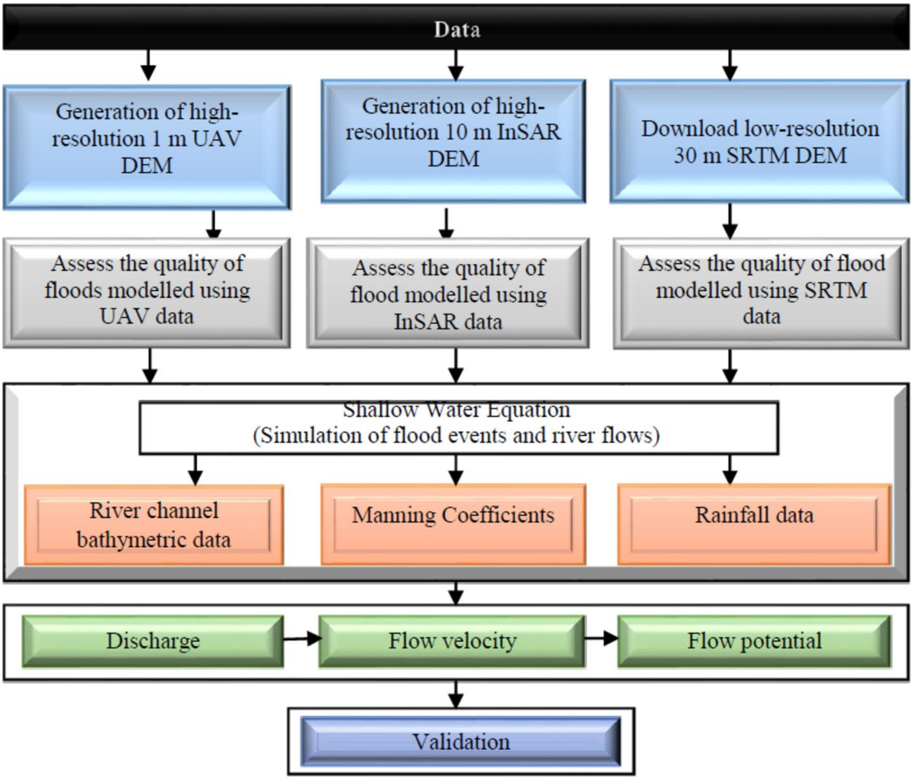

Fig. 1 The methodological workflow of the study

2.3 Data and Methods

2.3.1 Data Acquisition and Processing

Field surveys and historical documents were utilised in this study to collect vital hydrological, topographical, meteorological, and bathymetric data for the Shiroro floodplain. Rainfall, temperature, inflow, water level, and outflow (water discharge) were among the hydrological and meteorological indicators acquired through the Shiroro Dam Authority between 2001 and 2020 (Shiroro Dam Authority 2020). This historical dataset was a starting point for comprehending the hydrological regime's long-term trends and variability in the area.

In 2022, a detailed bathymetric survey mapping the river channel downstream of Shiroro Dam accurately depicted the study area's form and configuration of the bed. About 955 data points were collected at random intervals, ensuring a spatially representative dataset. The bar-check method was employed to calibrate the Hi-Target DH Light Echo Sounder used for depth measurements. This technique enhances the accuracy of the echo sounder data by comparing the measured depth to the actual depth and adjusting the sound velocity accordingly (Lurton 2010).

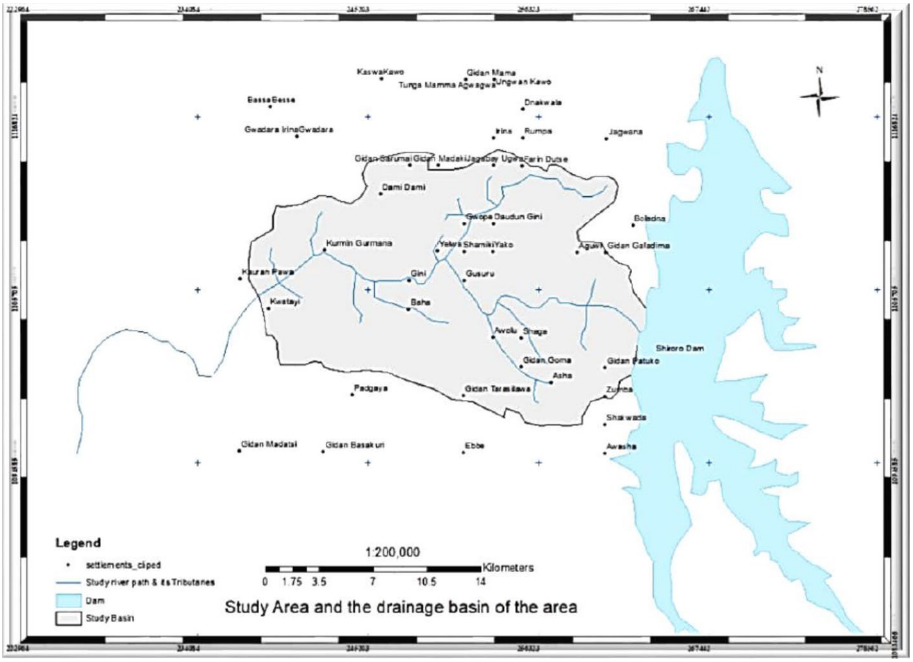

Fig. 2 Map of the study area

With its dual-frequency GPS receiver, the echo sounder made it easier to pinpoint the vessel's location and speed, which was essential for exact spatial reference of the bathymetric data. The instrument was standardized using parameters such as draft, ellipsoidal coordinates, time/date, frequency, velocity, and zone. The reference frame was based on the World Geodetic System (WGS 84) as the horizontal datum.

2.3.2 Generation of the DEMs

To evaluate the effect of resolution on flood modelling, this study utilised three distinct Digital Elevation Model (DEM) datasets: (i) a high-resolution (1 m) UAV-derived DEM, (ii) a 10 m resolution InSAR-generated DEM, and (iii) a 30 m SRTM DEM.

A 1 m Digital Elevation Model (DEM) was generated from UAV-captured images using a Trimble UX5 aerial imaging device and processed with the Trimble Business Centre Photogrammetry Module (Version 3.30). High positional accuracy was achieved through precise georeferencing, utilising 46 Ground Control Points (GCPs) (Ajayi et al. 2017). Table 2 presents the UAV mission's flight planning parameters, which clarify the data collection plan. Outlining the procedures for obtaining the topographic data from SAR interferometry.

The 10 m InSAR-derived DEM was generated using Sentinel Applications Platform (SNAP) version 8.0. The processing followed a standard workflow, which included data preprocessing, co-registration, interferogram generation, phase unwrapping, and geocoding. The approach was in line with accepted practices for processing InSAR data, making it easier to provide topographic data (Rosen et al. 2000). Figure 3 shows the data processing workflow for InSAR DEM creation.

Table 2 Flight planning parameters for the UAV mission

Parameter	Value
Flying height	200 m
Flight speed	12–15 m/s
Forward lap	70%
Side lap	65%
Camera focal length	24 mm
Flight time is approximately (Per flight)	15 min
Battery capacity	5350 mAH
Capacity of each image	6 megabytes
Number of GCPs	106 points
Number of GCPs used for georeferenced	60 points
Number of GCPs used for the adjustment of Tie points	46 points

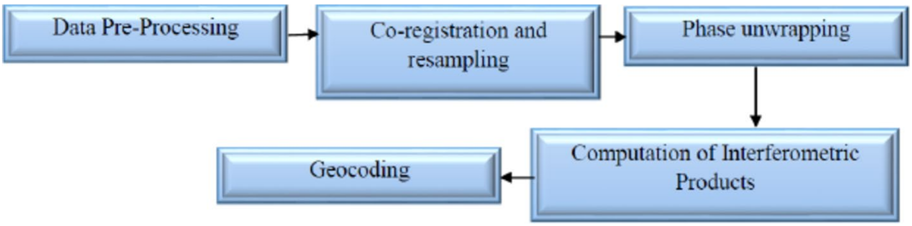

Fig. 3 InSAR data processing stage (Okeke 2006)

The 30 m SRTM data was obtained from the US Geological Survey website with a precision of 1 to 3 arc seconds, a worldwide accessible dataset produced using Spaceborne Imaging Radar-C technology. Although the relatively acceptable vertical accuracy of SRTM data on flat terrain makes it potentially useful for flood modelling, it also has drawbacks, such as invalid areas and, in the representation of a Digital Surface Model (DSM) rather than a bare-earth DEM (Farr et al. 2007; Slater et al. 2006). Since DSM representation includes vegetation and built-up characteristics, it may overestimate surface roughness and change flow path errors in flood modelling.

2.4 Methods

This study employed a methodology that integrated hydraulic analysis and topographic modelling to examine the interactions between river flow dynamics, surface topography, and climatic factors within the Shiroro floodplain. It created complex 3D flood simulations using Digital Elevation Models (DEMs) produced by various sources, including optical stereo imaging, aerial photography, and SAR interferometry. A two-dimensional hydrodynamic model was selected due to the inherent limitations of one-dimensional models in accurately representing flow across complex terrain. This model has proven to be much more effective at simulating flow patterns across the vast floodplain, which is in line with the results of earlier studies that emphasized the benefits of 2D models for floodplain simulation (Bates and De Roo 2000; Horritt and Bates 2002). River outflow and flow rates using Shallow Water Equations (SWEs) were first applied in MATLAB and then incorporated into flood simulations in ArcScene (ArcGIS 10.4). The considerable literature on hydraulic modelling supports SWEs, a widely accepted method for simulating free-surface flows (Chaudhry 2008; Toro 2001).

The impact of DEM resolution on hydrological and hydraulic modelling was evaluated using the three different DEM datasets: SRTM 30 m, InSAR 10 m, and UAV-derived 1 m. To understand surface water flow dynamics within the catchment, early hydrological assessments concentrated on determining basic hydrological characteristics, such as flow direction, flow accumulation, and watershed delineation. These hydrological characteristics are commonly used in flood modelling and watershed study (Maidment 2002; Tarboton 1997).

The SWEs is (Eqs. (1–6) were then implemented in MATLAB to model river discharge and flow velocity. Important input data, such as rainfall data, Manning coefficients, river channel bathymetric data, and the corresponding DEM datasets, were included in this application to improve the simulations' realism and accuracy. Several studies have shown that successful hydraulic modelling requires combining bathymetric data with Manning coefficients, which describe channel roughness (Chow 1959; French 1985). A strong and scientifically sound framework for evaluating flood risk within the Shiroro floodplain was achieved through this multifaceted methodological approach, which integrated various DEM sources and used hydraulic modelling techniques. This approach conformed with best practices in flood hazard assessment (Pappenberger et al. 2007; Werner et al. 2005).

$$\frac{\delta Q}{\delta t} + \frac{\partial}{\partial x}\left(\frac{Q^2}{A}\right) = -gAS_f + gAS_0 - gA\frac{\partial h_o}{\partial x} \tag{1}$$

where

Q = discharge

A = cross-sectional area

$\frac{\delta Q}{\delta t}$ = rate of discharge for time

$\frac{\partial}{\partial x}\left(\frac{Q^2}{A}\right)$ = rate of discharge with respect to cross-sectional area

g = acceleration due to gravity

S_f= frictional slope

S_o = reference slope

h_0 = is a typical length characteristic of the height of the flow

$\frac{\partial h_o}{\partial x}$ = channel bed-topography

Q can be computed as:

$$Q = \frac{A}{n} * R^{\frac{2}{3}} * S^{\frac{1}{2}} \tag{2}$$

where

R =Hydraulic radius

n =Manning coefficient of roughness

A = Cross-sectional area

S = Channel slope in the direction of flow,

$\frac{\partial h_o}{\partial x}$ is obtained from the bathymetric observation

A is measured from satellite imagery (width) and some points validated on the ground
S_f and S_o are deduced from the digital elevation model, and
Q is computed using Eq. (2)

Thus, the simultaneous substitution of the computed value of Q from Eq. (2) into Eq. (3) allows the calculation of the actual flow rate $\frac{\delta Q}{\delta t}$ in Eq. (1).

Again, Eq. (3) is used to compute the stream flow rate:

$$F_r\left(\frac{\partial h_0}{\partial x}\right) = \frac{A \times L \times C}{T} \tag{3}$$

where
F_r = flow rate
A = cross-sectional area.
L = length of reach
C = coefficient or correction factor to accommodate for the drag due to sediments and channel disturbance.
T = Time in seconds

Combining the water channel discharge capacity (Q) with the discharge rate ($\frac{\delta Q}{\delta t}$) and stream flow rate, the flooding potentials of the water channel was simulated using Eqs. (4), (5) and (6).

$$W_f = \frac{\delta Q}{\delta t} \times F_r \tag{4}$$

where
W_f = water flux
$\frac{\delta Q}{\delta t}$ = discharge rate

$$If \qquad W_f > Q \quad \text{River section is potentially flood prone} \tag{5}$$

$$W_f \leq Q \quad \text{River section is not potentially flood prone} \tag{6}$$

2.4.1 Statistical Analysis

Following established hydrological and geospatial modelling, statistical analysis was essential in quantifying the variations and connections across the DEM sources (Congalton and Green 2009). Standard deviation was used to evaluate the dispersion of elevation values within each DEM, and to reveal the inherent variability of the datasets, while Analysis of Variance (ANOVA) was used to determine if there were statistically significant differences in the mean elevations among the UAV, InSAR, and SRTM DEMs (Skidmore 1989). Also, Root Mean Square Error (RMSE) was used to quantify the discrepancies between simulated and observed flood extents by comparing the flood extents derived from each DEM with validation data, a commonly used metric in model evaluation (Chai and Draxler 2014), and correlation analysis was used to shed light on the parameters' constancy across various resolutions by examining the linear correlations between the hydrological and hydraulic parameters produced from the DEM. These methods were used to ensure a rigorous and objective evaluation of the DEMs and their impact on hydrological and hydraulic modelling within the Shiroro floodplain, while highlighting the influence of DEM resolution on model accuracy, with RMSE providing a critical quantitative measure of the differences between simulated and observed flood extents and depths (Legates and McCabe 1999).

2.4.2 Model Validation

Model validation is a crucial stage in any modelling study evaluating the simulations' dependability. It ideally involves directly comparing simulation findings with observed flood depths and extents by ground truthing or field verification, however, due to pervasive security threats in the study location, direct field validation was not feasible, resulting in reliance on damage estimates from previous research and data from the Niger State Emergency Management Agency (NSEMA). This allows for comparison of the model's performance to established scientific knowledge and verified flood consequences, acknowledging that reliance on secondary data for validation becomes necessary when direct field data is unavailable (O'Connell et al. 2010), and recognising the ambiguity and inherent limitations of secondary data.

2.4.3 Hydrological Regime Analysis

The hydrology of the Shiroro floodplain was characterised through a detailed analysis of 20 years of time-series data from the Shiroro Dam Authority, including monthly inflow, temperature, water level, and outflow, involving data collection and compilation into a structured database, temporal visualisation using time-series plots to identify patterns and trends, statistical analysis using descriptive statistics and Pearson's correlation displayed via matrices and scatter plots, seasonal pattern identification using monthly averages reflecting the influence of the West African monsoon, and data validation and quality control using interpolation when needed to maintain dataset integrity.

3 Results and Discussion

3.1 Hydrological and Topographical Data Analysis

3.1.1 Hydrological Characterization

The hydrological characteristics of the study area were analysed using time-series data, including average monthly inflow, temperature, water level, and outflow, as depicted in Fig. 4(a-e), illustrating the temporal variability of key hydrological metrics and revealing the water system's dynamics, while Fig. 5(a-e) presents the results of a Pearson's correlation analysis, examining the relationships between these variables and quantifying the direction and strength of linear correlations between temperature, inflow, outflow, rainfall, and water levels, thereby adding to a thorough understanding of the hydrological processes in the watershed.

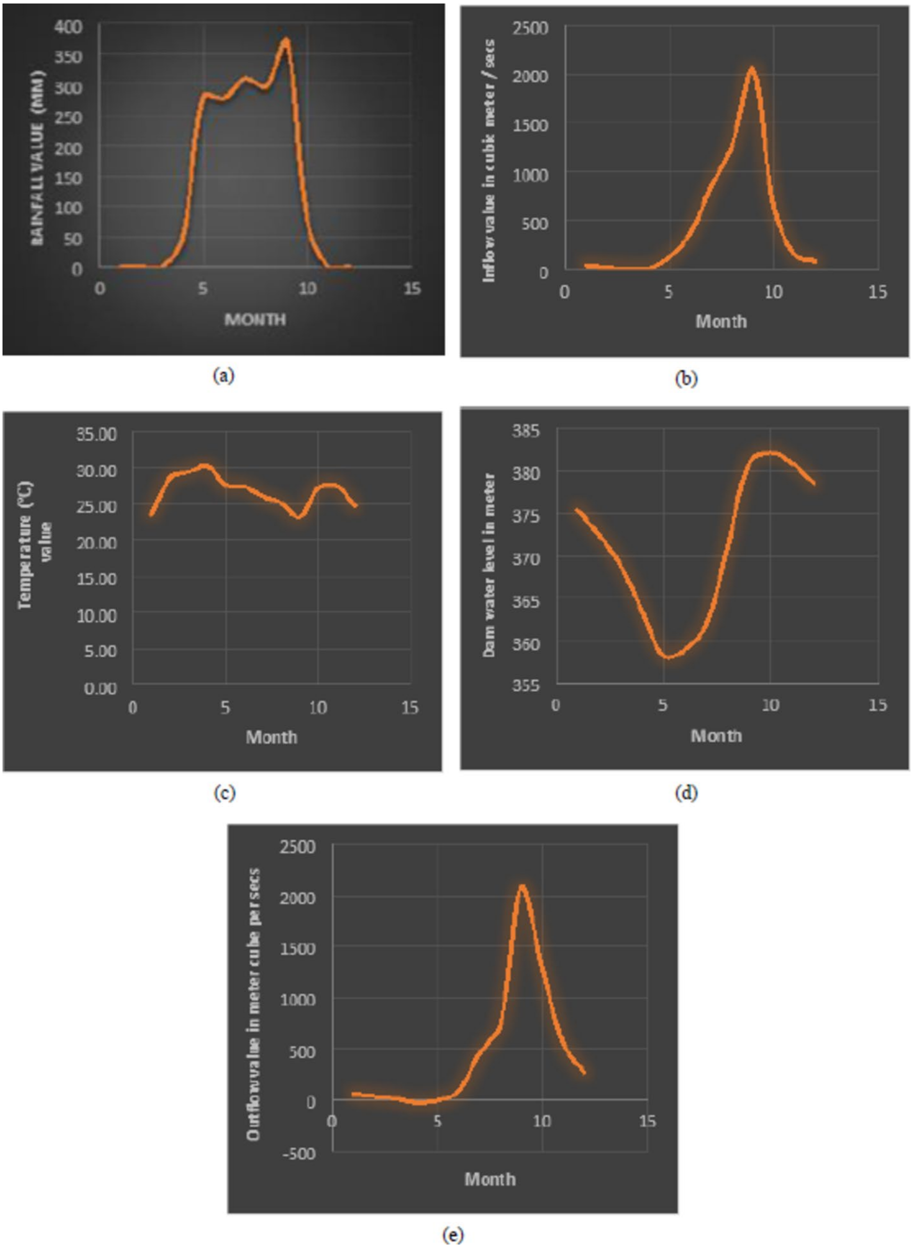

Fig. 4 **a** Average monthly rainfall data. **b** Average monthly inflow data. **c** Average monthly temperature data. **d** Average monthly water level data. **e** Average monthly outflow data

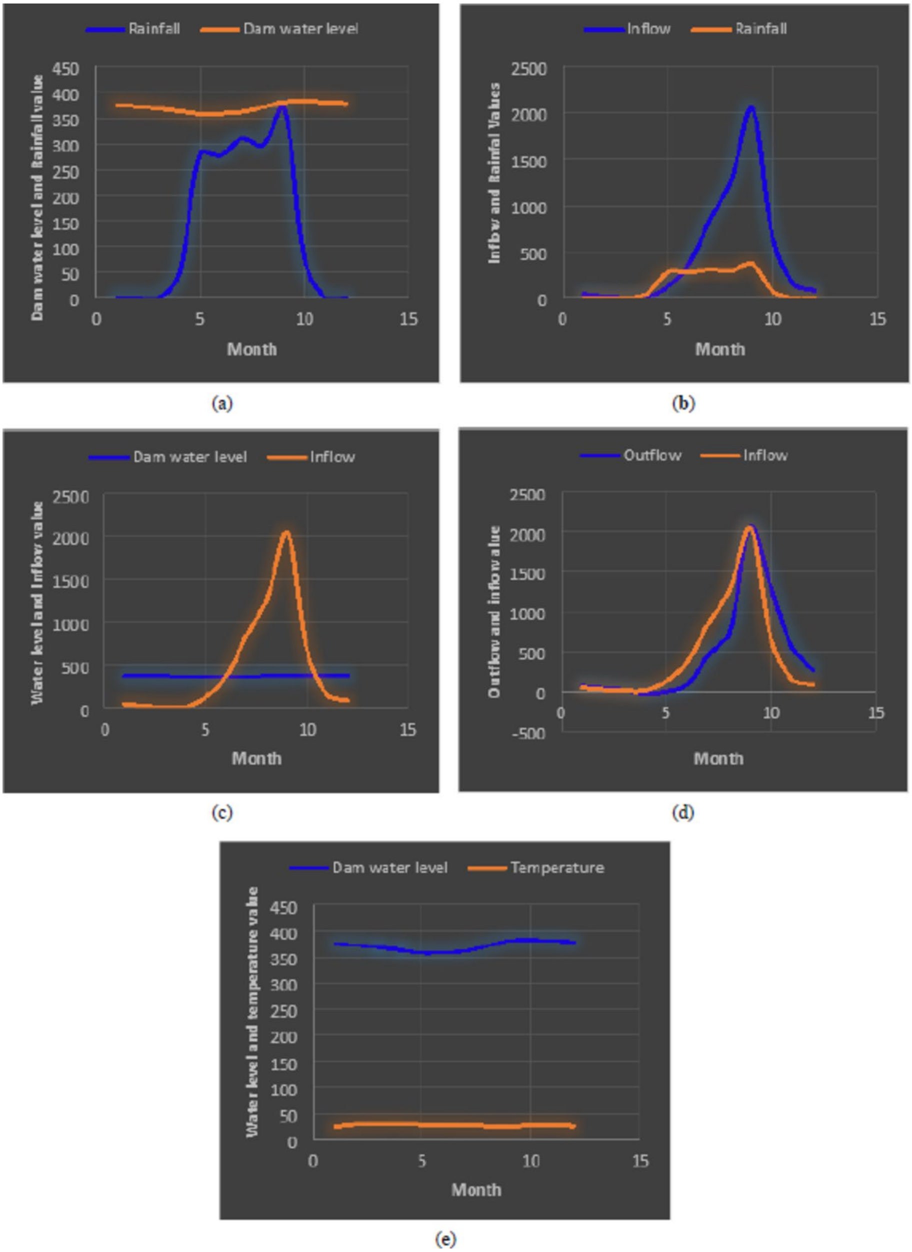

Fig. 5 **a** Dam water level data and Rainfall. **b** Inflow and rainfall data. **c** Water level and inflow data. **d** Inflow and outflow data. **e** Water level and temperature

Table 3 Summary of bathymetric information for the study area

Parameter	Value (m)
Minimum depth	0.95
Maximum depth	2.15
Average depth	1.20
Total number of points	955

Table 4 Descriptive statistics of the DEMs

Parameter	UAV (m)	InSAR (m)	SRTM (m)
Min	156.527	173.031	177.110
Max	601.679	635.599	665.032
Range	445.152	458.489	492.000
Average	323.903	348.594	357.991
Std dev	84.707	87.290	93.622

3.1.2 River Channel Bathymetry

A comprehensive bathymetric survey, encompassing 955 data points, was conducted on the downstream river channel of the Shiroro, yielding a detailed bathymetric profile that provides vital information on channel morphology which is essential for precise hydraulic modelling and flood risk assessment, with Table 3 presenting a quantitative summary of the channel's geometric properties through statistical descriptors of the bathymetric data, including measures of central tendency and dispersion.

3.1.3 DEM Evaluation and Comparison

The evaluation of three different Digital Elevation Models (DEMs) was conducted to assess their suitability for flood modelling, including a low-resolution 30 m SRTM DEM, a medium-resolution 10 m InSAR DEM, and a high-resolution 1 m UAV-derived DEM, validated by data from low- and high-settlement areas provided by the Niger State Emergency Management Agency (NSEMA), with this validation process aiming to determine the accuracy and reliability of each DEM in representing topography and its effect on flood inundation, and Table 4 displaying the descriptive statistics for each DEM, including the mean, standard deviation, minimum, and maximum values, providing a numerical comparison of their elevation characteristics, while Figs. 6(a-c) visually display the derived flow direction, watersheds, flow accumulation, and surface runoff for each DEM, facilitating a qualitative comparison of the hydrological outputs generated by the different DEM sources (Table 5).

3.1.4 Statistical Analysis of DEM Performance

A single-factor Analysis of Variance (ANOVA) was employed to statistically compare the performance of three Digital Elevation Models (DEMs), specifically testing the null hypothesis of no significant variations in elevation values between UAV 1 m, InSAR 10 m, and SRTM 30 m DEMs, subsequently, a further ANOVA was conducted to identify specific pairwise differences among the DEMs, with the resulting F-statistic, p-value, and degrees of freedom detailed in Tables 6, and a summary of these statistical descriptors provided in Table 5, and additionally, Pearson's correlation analysis was performed to quantify

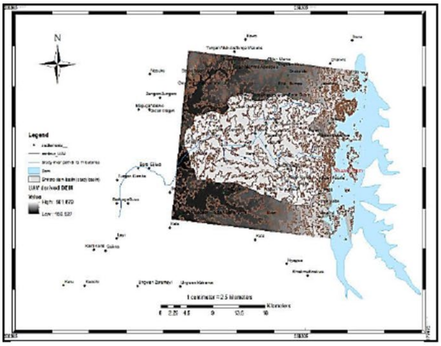

(6a) UAV 1 m DEM

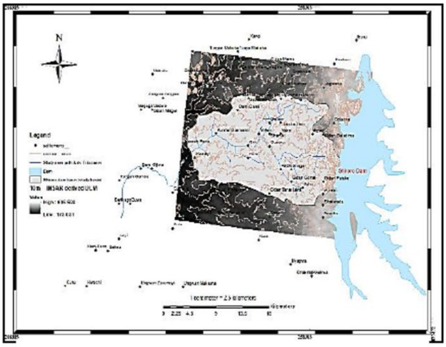

(6b) INSAR 10 m DEM

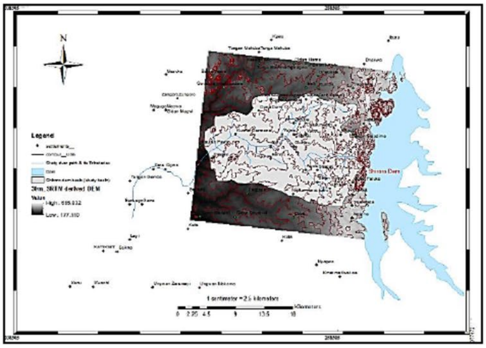

(6c) SRTM 30 m DEM

Fig. 6 Flow direction, watersheds, flow accumulation, and surface runoff when using the different DEM sources; (**a**) UAV 1 m (**b**) InSAR 10 m, and (**c**) SRTM 30 m

Table 5 ANOVA test (single factor) result table for the DEMs

Source of Variation	SS	DF	MS	F	*P*-VALUE	F-CRIT
Between Group	6199743.4	2	3,999,872	394.722	6.184 E- 170	2.996
Within Group	235,575,409	29,997	7853.299			
Total	241,775,152	29,999				

Table 6 ANOVA test (single factor) summary

Groups	Count	Sum	Average	Variance
UAV	10,000	3,239,034	323.903	7175.299
INSAR	10,000	3,485,940	348.594	7619.554
SRTM	10,000	3,579,913	357.991	8765.043

the linear relationships among the three DEMs, with the correlation coefficients presented in Table 7 revealing the degree of similarity and dissimilarity between the elevation data obtained from the respective sources.

3.2 Impact of DEM Resolution on Hydrological and Hydraulic Analysis

The hydrological analysis of the Shiroro floodplain revealed a notable sensitivity to DEM resolution, which demonstrates the differences in derived hydrological parameters. The flow direction and watershed borders obtained from the UAV, InSAR, and SRTM DEMs, shown in Fig. 7(a-c), respectively, illustrate the disparate spatial representation of drainage networks at various resolutions. Figure 8, which contrasts flow accumulation and surface runoff patterns, emphasizes these distinctions even further and shows how DEM resolution affects the measurement of water flow channels.

Table 8 presents the quantification of the effect of DEM resolution on variables like drainage density and basin area, representing the main morphometric features of the river basins. These results are consistent with the established principle that DEM resolution directly impacts the quality of derived hydrological parameters, influencing surface topography and water flow simulation (Tarboton 1997; Wilson and Gallant 2000).

The research expanded to examine how DEM resolution affects hydraulic analysis. The discharge rate, flow velocity, and elevation profiles obtained from the three DEMs are visually depicted in Fig. 9(a-c), with variations in hydraulic characteristics at various resolutions. The discharge rate, flow velocity, and elevation variances between the DEMs are in Figs. 10(a-c) to enhance understanding of these fluctuations and demonstrate the extent of the inconsistencies caused by resolution variations.

These findings align with the established influence of DEM resolution on hydraulic modelling, wherein more detailed channel geometry and flow dynamics are represented by higher-resolution DEMs, resulting in more precise hydraulic parameter estimates (Horritt and Bates 2002; Merwade et al. 2008). The observed disparities highlight the importance of selecting appropriate DEM resolutions for hydrological and hydraulic assessments, particularly in flood-prone areas, where precise flow channel and hydraulic parameter representation is essential for effective risk assessment and management.

3.3 Flood Risk Assessment and Vulnerability Analysis

3.3.1 Catchment Characterization and Hydraulic Modelling

The study area is defined by Twelve (12) contributing water channels, which covers a catchment of 466.995 km² within a larger drainage basin of approximately 2000 km², indicating a relatively low downstream slope. Hydraulic modelling was employed to evaluate flood risk using river bathymetry and the three Digital Elevation Models (DEMs), with MATLAB processing implementing a hydraulic equation to calculate flood levels at specific nodes along these channels, following the methods described in Adesina et al. (2021) (Eq. 1 to 6), and

Table 7 Correlation analysis of the DEMs

DEM	InSAR (10 m)	SRTM (30 m)	UAV (1 m)
InSAR	1		
SRTM	0.999639	1	
UAV	0.999639	0.999524	1

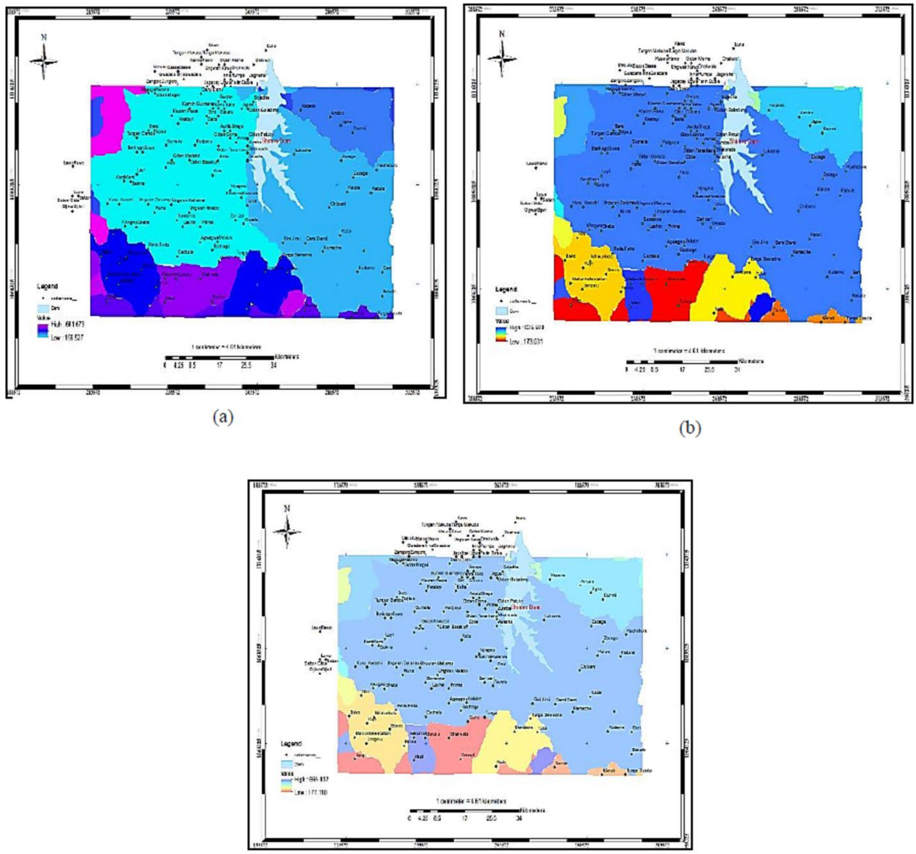

(a) (b) (c)

Fig. 7 **a** Watershed generated from UAV 1 m DEM. **b** Watershed generated from InSAR 10 m DEM. **c** Watershed generated from SRTM 30 m DEM

applying an initial discharge boundary condition of 114.38 m³/s. The details of the resulting discharge, flow velocity, and water surface heights at each node is presented in Table 9.

3.3.2 Comparative Analysis of Flood Inundation Extents

The hydraulic modelling revealed significant differences in the expected flood inundation extents among the three DEMs (Figs. 11a-c), with the UAV-derived 1 m DEM predicting flood heights ranging from 150 to 250 m, the InSAR 10 m DEM estimating higher flood levels between 160 and 270 m, and the SRTM 30 m DEM predicting the most extensive inundation with flood heights ranging from 200 to 280 m, potentially submerging the floodplain. Table 10 outlines the population figures of the communities affected by these anticipated flood levels.

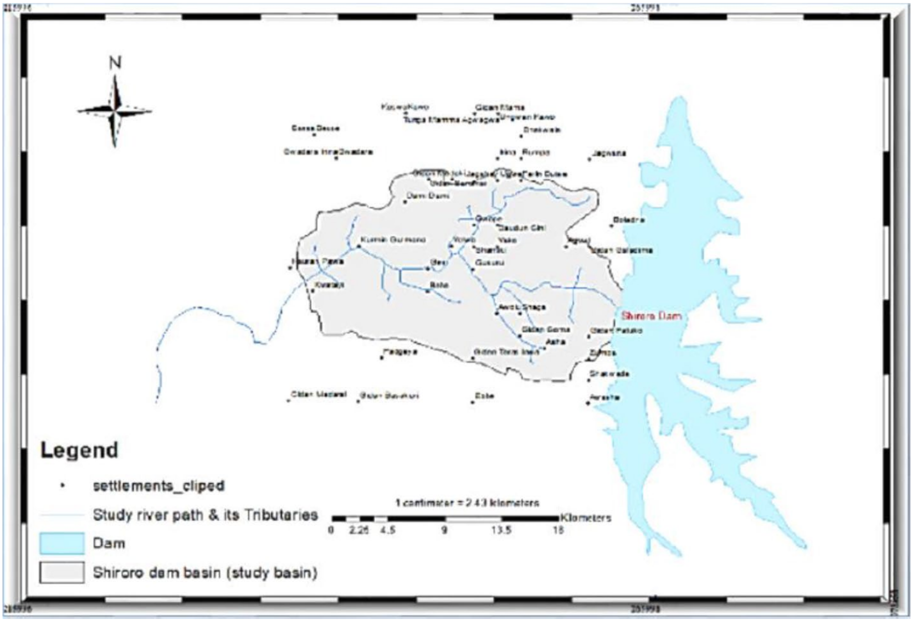

Fig. 8 Delineated catchment area from DEMs

Table 8 Summary of the study area's hydrological characteristics

Hydrological Parameter	UAV 1 m DEM	InSAR 10 m DEM	SRTM 30 m DEM
Total no of basins	14	10	13
No major basins	6	6	8
Size of the largest basin	(43.5 by 30.2) km	(42.8 by 30.8) km	(34.7 by 30) km
Size of smallest basin	(6.6 by 12.4) km	(6.1 by 3.9) km	(4.7 by 3.98) km
No runoff streams/tributaries	Same network	Same network	Same network

3.3.3 Flood Vulnerability Mapping and Spatial Analysis

Flood vulnerability maps were created for each DEM in the ArcScene environment, illustrating the spatial distribution of potential inundation (Figs. 12a-c), with lighter blue tones representing lower risk and darker blue tones indicating higher vulnerability the results effectively demonstrate the spatial variability of flood risk and identifying critical hotspots and assessing potential impacts on infrastructure and communities.

3.3.4 Validation and Accuracy Assessment

The validation and accuracy assessment compared the anticipated flood inundation extents with historical flood data from the Niger State Emergency Management Agency (NSEMA) revealed that the 1 m DEM produced by the UAV accurately represented ground conditions

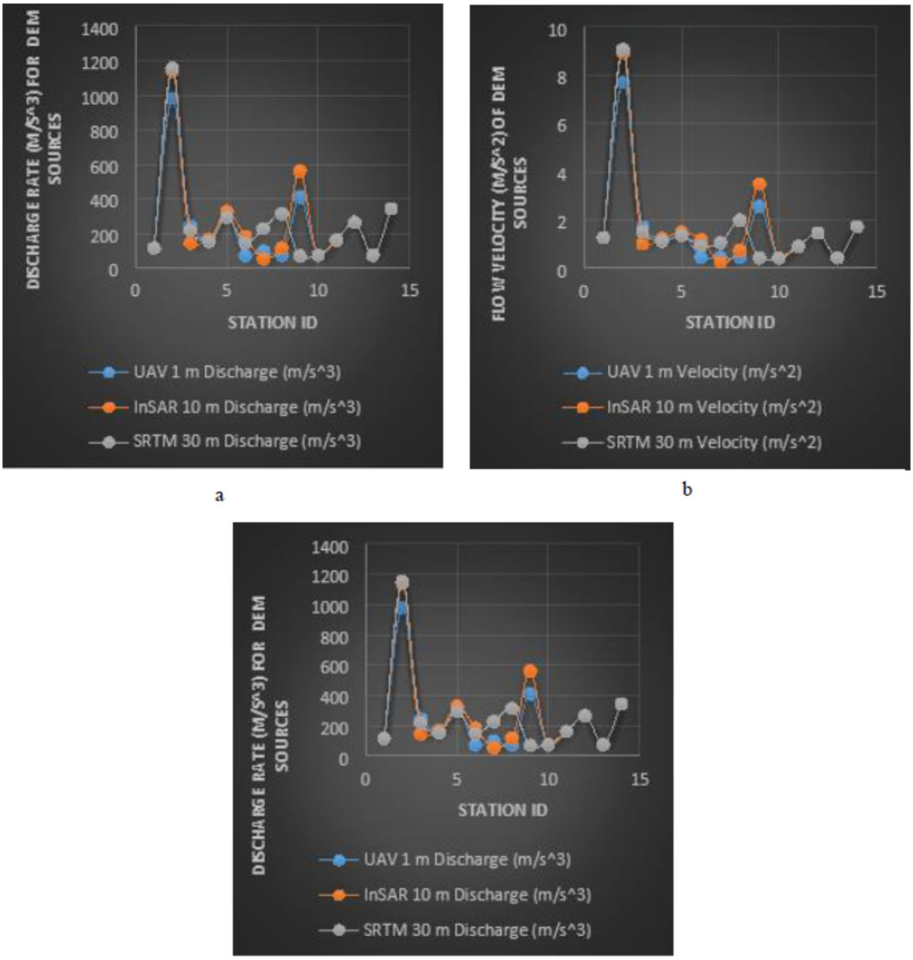

c

Fig. 9 **a** Discharge rate from DEM sources. **b** Flow velocity from the DEM sources. **c** Elevation from DEM sources

and closely matched historical flood data. In comparison, the 30 m SRTM and the 10 m InSAR DEMs tend to overestimate flood risk, primarily due to their inherent data limitations and lower spatial resolution.

3.4 Flood Vulnerability Mapping and Inundation Analysis

Figure 13(a-c) presents the weighted overlay maps depicting the spatial distribution of flood risk within the Shiroro floodplain. These maps illustrate areas vulnerable to flooding, produced using UAV (1 m), InSAR (10 m), and SRTM (30 m) DEMs. These maps, produced using a multi-criteria evaluation method, show the different levels of vulnerability according to the different DEM resolutions. Tables 11 and 12 provide a quantitative assessment of

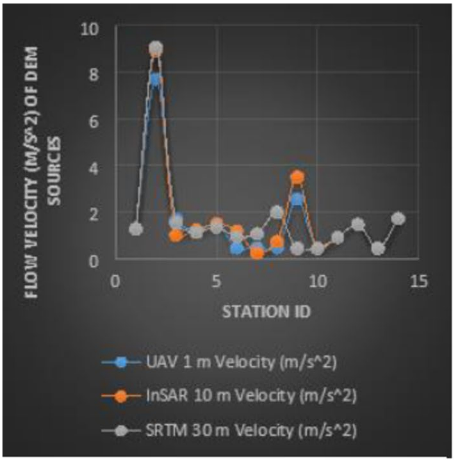

a

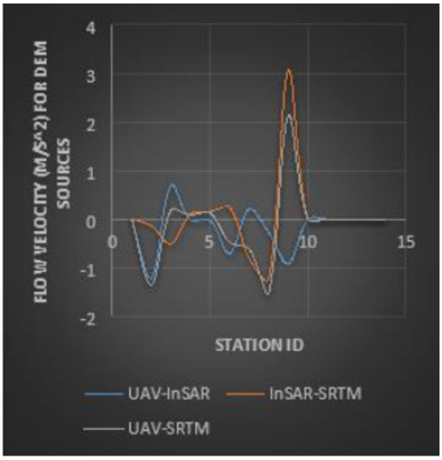

b

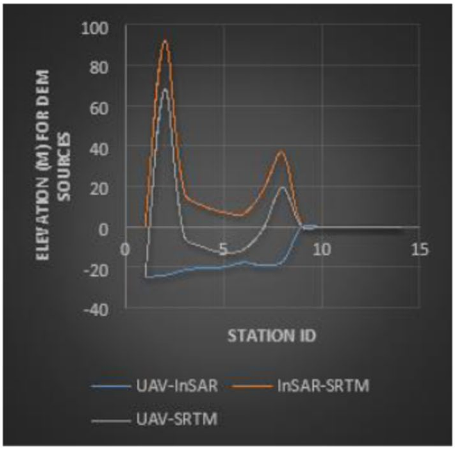

c

Fig. 10 **a** Discharge rate difference between DEMs. **b** Flow velocity difference between DEMs. **c** Elevation difference between DEMs

vulnerability by describing individual communities in danger of flooding at different flood heights, which helps to provide additional context for these spatial representations.

The choice of certain flood heights for each DEM reflects the intrinsic variations in topographic representation, which aligns with some of the findings on the effect of DEM resolution on flood modelling accuracy (Bates et al. 2010; Lane et al. 1998). Table 11 shows the flooding extents at 150 and 250 m for the UAV-derived 1 m DEM, illustrating the finer-scale variability in inundation patterns made possible by the high-resolution data. On the other hand, to accurately depict inundation extents, the InSAR-derived 10 m DEM, which has a poorer spatial resolution, requires the usage of 160 m and 270 m (Table 12) flood heights.

Similarly, based on the SRTM 30 m DEM, Table 13 shows flooding at 200 m and 280 m, illustrating the generalized inundation patterns and flattened terrain linked to low resolutions. Because it accounts for the inherent variations in topographic representation and

Table 9 Discharge rate and flow velocity using different DEM source

		UAV 1 m DEM			InSAR 10 m DEM			SRTM 30 m DEM		
Sta_ID	Settlement Name	Elevation (m)	Discharge (m/s^3)	Velocity (m/s^2)	Elevation (m)	Discharge (m/s^3)	Velocity (m/s^2)	Elevation (m)	Discharge (m/s^3)	Velocity (m/s^2)
A01	Gidan Patuko	348.46	114.38	1.27	373.32	114.38	1.27	373.07	114.38	1.27
A02	Gidan Patuko	348.16	982.14	7.71	372.12	1137.03	8.93	280.09	1154.42	9.07
A03	Awolu Saga	251.16	244.82	1.71	272.64	144.72	1.01	256.09	219.00	1.53
A04	Sumaila	212.97	164.32	1.20	233.35	166.67	1.22	223.20	152.48	1.12
A05	Bere	198.36	322.99	1.48	218.35	327.25	1.50	211.10	293.92	1.35
A06	Tungan-Gamba	197.93	71.75	0.46	215.55	183.46	1.18	209.33	146.16	0.94
A07	Layi	195.72	96.68	0.45	214.86	53.80	0.25	197.05	227.45	1.06
A08	Nill	194.53	72.83	0.46	211.86	115.79	0.74	174.97	314.13	1.99
A09	Nill	174.39	411.48	2.56	174.39	561.24	3.49	174.39	69.90	0.43
A010	Nill	174.30	73.83	0.43	175.32	74.63	0.61	176.23	74.73	0.73
A011	Nill	167.08	161.14	0.91	167.08	161.14	0.91	167.08	161.14	0.91
A012	Nill	159.30	264.57	1.46	159.30	264.57	1.466	159.30	264.57	1.46
A013	Lawo Ravo	159.12	73.96	0.43	159.12	73.96	0.43	159.12	73.96	0.43
A014	Nill	128.00	343.64	1.72	128.00	343.64	1.72	128.00	343.64	1.72

enables a more nuanced understanding of flood risk dynamics, different flood heights across DEM resolutions are essential for comparison research. This strategy is in line with flood hazard assessment best practices, which stress the significance of considering the constraints of input data and implementing suitable procedures to reduce uncertainty (Merwade et al. 2008).

3.5 Model Validation Results

Notable performance variations were observed among the tested DEM resolutions when flood extent predictions were validated against historical data from the Niger State Emergency Management Agency (NSEMA) and compared with results from previous studies (Leitao et al. 2016; Esmaeel et al. 2022). With consistent agreement with observed ground conditions, the UAV-derived 1 m DEM showed the most accurate representation of flood inundation, as shown in Fig. 14. This concordance emphasizes the vital importance of high-resolution topographic data in capturing the complex spatial patterns of flood episodes, in line with accepted guidelines for geomorphological flood modelling (Horritt and Bates 2002).

On the other hand, there were notable differences between the 10 m InSAR and 30 m SRTM DEMs flood extent prediction, underscoring the shortcomings of low-resolution data in capturing the terrain of the Shiroro floodplain. According to Merwade et al. (2008), these

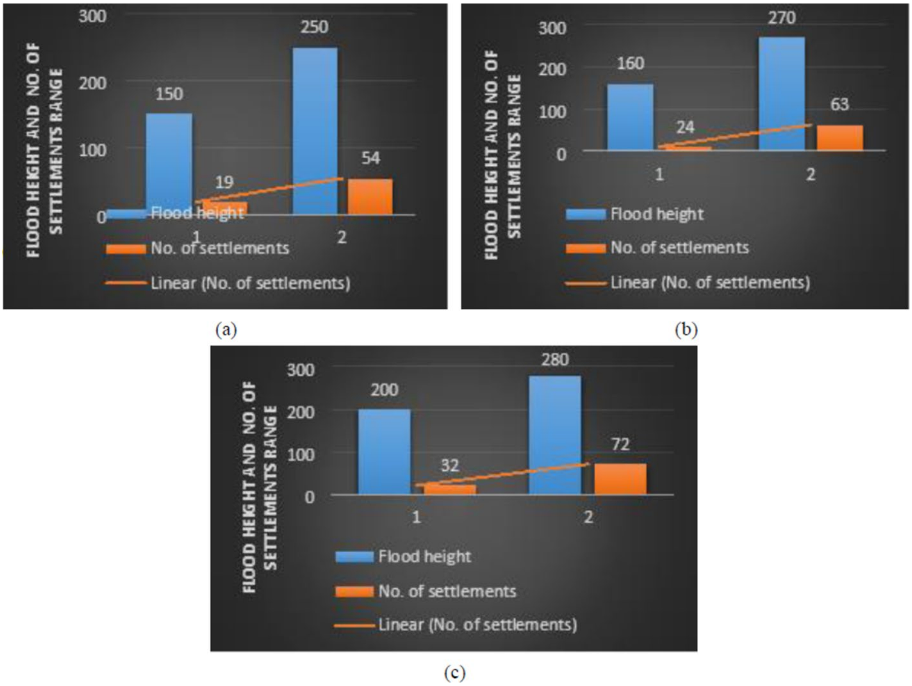

Fig. 11 **a** Flood height based on UAV 1 m DEM at 150 m and 250 m. **b** Flood height of InSAR 10 m DEM based on 160 m and 270 m. **c** Flood heights of 30 m based on SRTM DEM at 200 m and 280 m

Table 10 Number of flood-prone settlements using different DEM sources

UAV 1 m DEM		InSAR 10 m DEM		SRTM 30 m DEM	
Flood heights	Vulnerable settlements	lood heights	Vulnerable settlements	Flood heights	Vul-nerable settle-ments
150 m	20	160 m	24	250 m	32
250 m	57	270 m	63	280 m	72

disparities align with the known sensitivity of flood inundation models to DEM resolution, where lower resolution data tends to generalize topographic characteristics, resulting in inaccurate flood extent delineation.

In flood hazard assessment, scale and resolution are crucial. The observed agreement of the 1 m UAV DEM with NSEMA's data and previous studies highlights the necessity of high-fidelity topographic data for effective flood risk management. The disparities seen with the lower-resolution DEMs also demonstrate how using such data can lead to substantial errors in flood inundation mapping, potentially resulting in insufficient or inadequate flood protection measures.

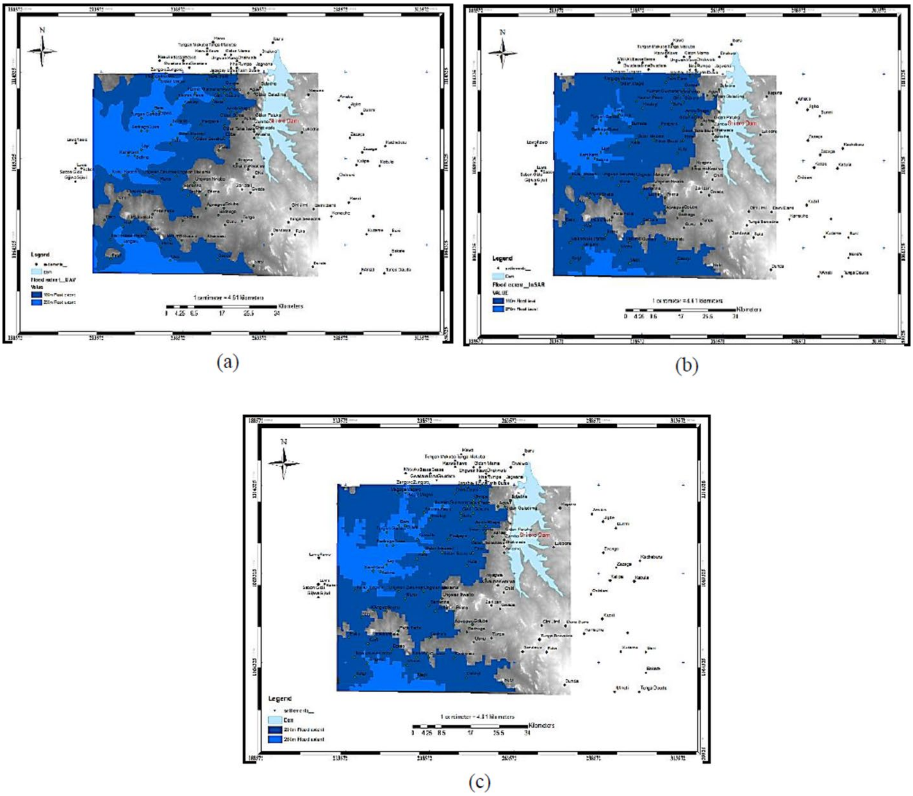

Fig. 12 **a** UAV-derived 1 m DEM vulnerability flood extents. **b** InSAR 10 m DEM vulnerability flood extents. **c** SRTM 30 m DEM vulnerability flood extent

3.6 Discussion

The impact of different Digital Elevation Model (DEM) resolutions on flood risk assessment in Nigeria's Shiroro floodplain was thoroughly investigated in this study. The hydrological data analysis, including rainfall, inflow, temperature, reservoir water levels, and outflow (Fig. 4a and e), showed a clear seasonal pattern typical of the monsoon climate in West Africa, as substantiated by Bijan et al. (2024). The region's flood risk is influenced by a complex interplay of hydrological and meteorological factors, as evidenced by the observed correlation between rainfall and inflow (Gaurav et al. 2024), the inverse relationship between temperature and precipitation (Dadiyorto et al. 2019), and the ensuing fluctuations in reservoir water levels and outflow (Yudai et al. 2024; Spina et al. 2025; Xuefei et al. 2016).

Understanding the dynamics of the Shiroro Dam reservoir was strengthened by additional examination of Fig. 4a and e. The direct correlation between inflow and water elevation (Syed et al. 2024), the substantial contribution of upstream catchment runoff to inflow (Gaurav et al. 2024), the elevated water levels during the rainy season (Yaru et al. 2024; Kim et al. 2024), and the storage variations reflecting typical dam operational dynamics (Ahmed et al. 2023) all conformed to accepted hydrological principles (Fig. 5a and e). More

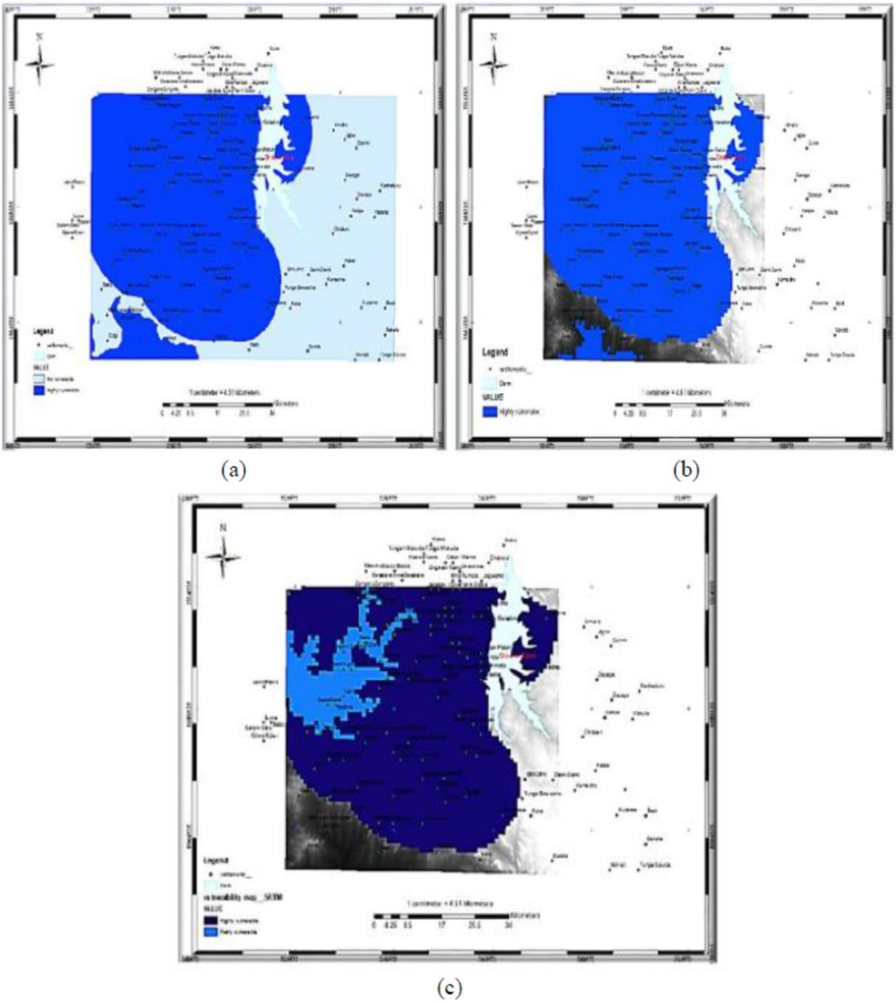

Fig. 13 **a** Weighted overlay of the flood-vulnerable area from UAV-derived 1 m DEM. **b** Weighted overlay of the flood-vulnerable area from InSAR 10 m DEM. **c** Weighted overlay of the flood-vulnerable area from SRTM 30 m DEM

research should be done on the relationship between low temperatures and higher water levels, which may be less evaporation (Hannes et al. 2024). The significance of efficient reservoir management techniques was highlighted by the impact of spillway gate operations on downstream flooding (Syahida et al. 2023), the possible correlation between increased temperatures and decreased rainfall (Mohamed et al. 2022), and the larger context of dam-induced downstream impacts (Adesina et al. 2022; Yousra et al. 2021; Muyuan et al. 2023; Desmond et al. 2024).

A solid approach for calculating discharge volume, rate, and flow velocity was generated by integrating river channel bathymetry data (Table 3) with DEM sources and the Shallow Water Equations (SWE) in MATLAB (Vinh and Jongho 2024). The importance of using

Table 11 Vulnerable settlements by UAV 1 m DEM flood heights

Flood height 150 m	Flood height 250 m		
Bere	Bere	Kwatayi	Gijiwa
Samboro	Samboro	Baha	Samboro
Berikago	Berikago	Kafa	Berikago
Guwa	Guwa	Gidan Basakuri	Manta
Sumaila	Sumaila	Ebbe	Sumaila
Gidan Madatsi	Gidan Madatsi	Gidan Tarasilawa	Gidan Madatsi
Seikna	Seikna	Padgaya	Seikna
Jiko	Jiko	Awolu	Jiko
Manta	Manta	Shaga	KamiKamt
KamiKamt	KamiKamt	Lashin	Jangaru
Jangaru	Jangaru	Ungwan	Mapi
Layi	Layi	Zarumayi Ungwan	Tungan
Tungan	Tungan	Kuyi	Kwochi
Gijiwa	Gijiwa	Bosso	Numbupi
Kwochi	Kwochi	Minna	Baganakwo
Wuna	Wuna	Daboyi	ShalukoShalko
Baganakwo	Baganakwo	Epigi	
Shaluko Shalko	shalukoShalko	Matumbi	
Mapi	Mapi	Samanna	
Numbupi	Numbupi	Kunu	

the DEM for flood modelling was demonstrated by NSEMA data (Fig. 14) (Sanaz et al. 2023; Hengkang and Yangbo 2024). The spatial resolutions and absolute elevation values of UAV, InSAR, and SRTM DEMs varied significantly, according to a comparative analysis (Figs. 6a–c; Table 4). Radar band differences, the nature of the SRTM surface model, and vegetation/terrain influences significantly contributed to the lower absolute elevation values of the UAV data when compared to InSAR and SRTM (Adesina et al. 2021; Xingyu et al. 2024).

The sensitivity of hydrological features to DEM accuracy and resolution was determined by the ANOVA test (Tables 5, 6 and 7) and hydrological analysis (Figs. 6a-c). The RMSE analysis (Figs. 9a-c; Table 9) and the examination of discharge and flow velocity differences (Figs. 10a-c; Table 9) demonstrated a stronger correlation between UAV and InSAR data than between UAV and SRTM. Vulnerability maps (Fig. 12a and c) show the areas affected by floods due to reservoir overflow, whereas flood height analysis (Table 10; Fig. 11a-c) showed the numbers of settlement impact at different flood levels. Figure 13a and c, which are weighted overlay maps of flood-prone areas, showed how well the high-resolution DEM obtained from UAVs could detect localized risky areas while capturing important micro-topographic features (Gafurov 2021). According to Sanaz et al. (2023), the smoother SRTM DEM underestimated floods in complicated terrain, while the UAV map's significant correlation with NSEMA data (Fig. 14) supported its better reliability.

The accuracy of flood inundation extent and depth estimates was directly impacted by the smoothing of subtle topographic features, which was a manifestation of the observed limitations of lower-resolution DEMs, specifically SRTM (30 m resolution, 177.110 m mean ele-

Table 12 Vulnerable settlements by InSAR 10 m DEM flood heights

Flood height 160 m	Flood height 270 m		
Gidan Magwi	Madaka Makuri	Kwatayi	Bere
Samboro	Kakuri	Baha	Gijiwa
Berikago	Maguga	Kafa	Sumaila
Guwa	Dami Dami	Gidan Basakuri	Jiko
Tungan Gamba	Kwatayi	Ebbe	Manta
Mapi	Kakuri	Baganakwo	Jangaru
Bere	Gijiwa	Ungwan Makama	Kami-Kamt
Gijiwa	Baha	Lashin	Seikna
Sumaila	Gusuru	Samanna	Gidan Madatsi
Jiko	Gurmana	Bosso	Kwochi
Manta	Yelwa	Minna	Layi
Kurmin	Gini	Shaluko Shalko	Tungan
KamiKamt	Yako	Ungwan	Daboyi
Seikna	Gwope	Zarumayi Ungwan	Epigi
Gidan Madatsi	Awolu	Kuyi	Tungan
Kwochi	Shaga	Gidan Magwi	
Layi	Padgaya	Samboro	
Kakuri	Wuna	Numbupi	
Wuna	Gidan Tarasilawa	Berikago	
Jangaru	Ebbe	Guwa	
Baganakwo	Gidan Basakuri	Tungan Gamba	
Shaluko Shalko	Kafa	Mapi	
Numbupi	Ungwan Zarumayi	Kurmin	
Gini	Jangaru	KamiKamt	

vation) and InSAR (10 m resolution, 173.031 m mean elevation). The higher performance of the UAV-derived DEM (1 m resolution, 156.527 m mean elevation) clearly illustrates the urgent need for sophisticated terrain representation. This result aligns with earlier studies that showed how crucial high-resolution topographic data is for precise flood modelling (Leitao et al. 2016; Esmaeel et al. 2022). Additionally, the study found that the "top of canopy" depiction of SRTM combined with errors introduced during DEM data gathering and processing led to notable differences in elevation measurements, which in turn, impacted hydrological studies. The RMSE comparisons (UAV-InSAR 0.352 m, UAV-SRTM 0.455 m, and UAV-NSEMA 0.249 m) highlight the need for thorough pre-processing and error correction processes by objectively validating the improved accuracy of the UAV DEM.

The study found the possibility of hydrological modelling errors in addition to DEM-related issues. Variations in discharge and flow velocity estimations, which by variables like the accuracy of rainfall data, channel roughness, and SWE model restrictions, served as an example of these inaccuracies. As demonstrated by the determined discharge volume, rate, and flow velocity, the critical importance of river channel bathymetry data in this context emphasizes the direct influence of bathymetric errors on discharge estimates, reaffirming the necessity of accurate channel representation. Future studies in the Shiroro floodplain and similar regions should focus on integrating high-resolution DEMs, like information

Table 13 Vulnerable settlements by SRTM 30 m DEM flood heights

Flood height 200 m	Flood height 280 m		
Samboro	Madaka Makuri	Ungwan Makama	Daboyi
Bere	Kakuri	Lashin	Epigi
Gijiwa	Maguga	Samanna	Tungan
Tungan Gamba	Dami Dami	Bosso	Berikago
Berikago	Kwatayi	Minna	Guwa
Guwa	Kakuri	Shaluko Shalko	Kunu
Gijiwa	Gijiwa	Ungwan	Maikunke
Layi	Baha	Zarumayi Ungwan	Samana
Jiko	Gusuru	Kuyi	Prinna
Manta	Gurmana	Gidan Magwi	Asha
KamiKamt	Yelwa	Samboro	Mukama
Seikna	Gini	Numbupi	Nabi
Baganakwo	Yako	Berikago	
Baha	Gwope	Guwa	
KamiKamt	Awolu	Tungan Gamba	
Seikna	Shaga	Mapi	
Gidan Madatsi	Padgaya	Kurmin	
Kwochi	Wuna	KamiKamt	
Layi	Gidan Tarasilawa	Bere	
Kakuri	Ebbe	Gijiwa	
Wuna	Gidan Basakuri	Sumaila	
Jangaru	Kafa	Jiko	
Baganakwo	Ungwan Zarumayi	Manta	
Shaluko Shalko	Jangaru	Jangaru	
Numbupi	Kwatayi	KamiKamt	
Gini	Baha	Seikna	
Dami Dami	Kafa	Gidan Madatsi	
Kwatayi	Gidan Basakuri	Kwochi	
Kakuri	Ebbe	Layi	
	Baganakwo	Tungan	

acquired from UAVs, to reduce these complex sources of error. Adopting strict DEM quality control procedures, using sophisticated hydrological modelling techniques, integrating various data sources, performing thorough sensitivity analysis, rigorously validating and calibrating models using independent datasets such as NSEMA data, quantifying uncertainty using sophisticated bathymetry data collection methodologies, and looking into the use of advanced SWE versions are also crucial. Thorough, data-driven methods like this, which are directly influenced by the results of the current study, will improve the validity and relevance of flood risk assessments in the Shiroro floodplain, leading to better flood control measures.

In line with the recognition of DEM sensitivity (Esmaeel et al. 2022; Bounab et al. 2022; Xingyu et al. 2024; Ozdemir and Akbas, 2015), the Shiroro floodplain study unequivocally establishes the critical influence of DEM resolution on flood risk assessment, reaffirming the established importance of high-resolution data (Leitao et al. 2016) and expanding this understanding by quantifying the limitations of low DEMs (InSAR, SRTM), which fail to

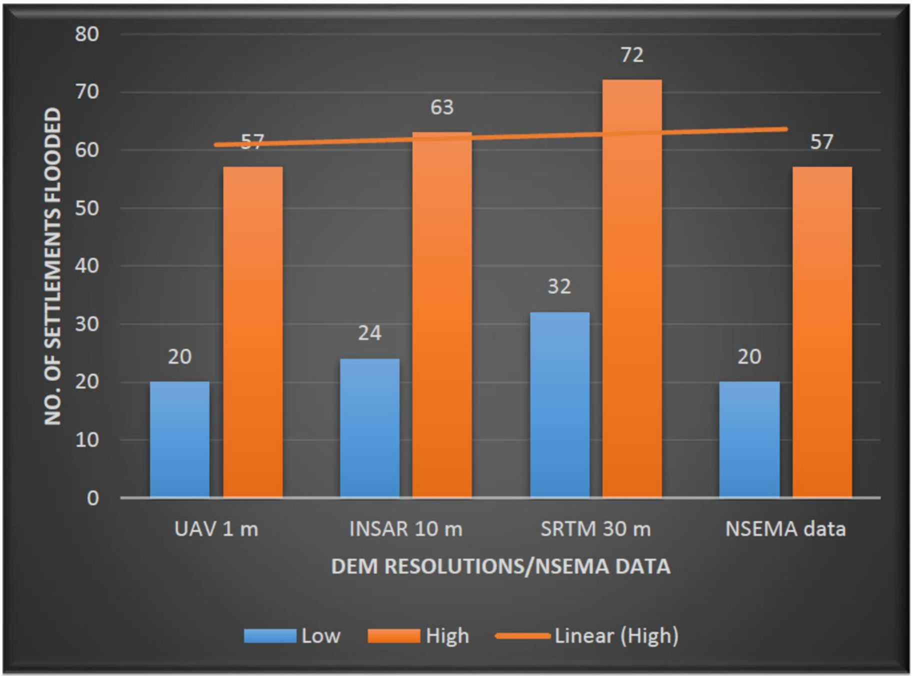

Fig. 14 UAV-derived DEM 1 m conformity with NSEMA 2022 data

capture detailed terrain features necessary for accurate flood modelling. According to the study, topographic smoothing in lower-resolution datasets causes an overestimation of flood inundation depth and area, which is directly correlated with decreasing DEM resolution. As demonstrated by its lower RMSE (0.249 m) in comparison to InSAR (0.352 m) and SRTM (0.455 m), the 1 m UAV-derived DEM offered the most accurate representation of flood extent, matching NSEMA historical data and displaying a distinct hazard distribution. This objective validation confirmed the crucial role that high-resolution UAV data plays in ensuring accurate flood risk assessment and management in the Shiroro floodplain.

4 Conclusion

This study emphasizes the vital role of high-resolution DEMs in enhancing flood risk assessment and guiding effective flood mitigation strategies, including early warning systems, evacuation planning, and resilient infrastructure in the Shiroro floodplain. The findings have significant implications for flood risk management in the Shiroro floodplain and beyond. High-resolution datasets provide valuable insights for decision-makers in several key areas. Firstly, they improve flood forecasting and early warning systems by Enabling timely alerts to affected communities, allowing for proactive evacuation and emergency response measures. Secondly, they facilitate the refinement of flood hazard maps and zoning by enabling the creation of more precise flood hazard maps, delineating areas at high risk of inundation. This information can be used effectively for land-use planning, building codes, and infrastructure development to reduce flood impacts. Thirdly, they enable the targeting of flood mitigation measures by identifying areas at high risk, allowing for the targeted implementation of flood mitigation measures, such as the construction of levees, floodwalls, and improved drainage systems. Finally, they improve disaster preparedness and response by enhancing the effectiveness of disaster preparedness and response plans, ensuring that resources are allocated efficiently and effectively during flood events.

Author Contributions All authors participated in the study's conception and design. EAA took the lead in material preparation and data collection and conducted the analysis. JOO and OGA contributed to the review and editing of the manuscript, and AM, ICO, and ARA provided supervision and contributed to the review and editing of the manuscript. EAA wrote the first draft of the manuscript, and all authors commented on previous versions. All authors read and approved the final manuscript.

Funding The authors declare that no funds, grants, or other support were received during the preparation of this manuscript.

Data Availability Data will be made available on request.

Declarations

Ethical Approval This paper has not been previously published and is not currently under review for publication in any other journal.

Consent to Participate The authors were involved in developing and submitting this paper for publication in Water Resources Management.

Consent to Publish All authors consent to the publication of this manuscript in Water Resources Management, confirming it is original and not under consideration elsewhere.

Competing Interests The authors have no relevant financial or non-financial interests to disclose.

References

Abayomi KI, Murtala AI, Babatunde O, Suleiman A (2015) Trend analysis of Hydro-Meteorological data for river Kaduna at Shiroro dam site, Niger State, Nigeria. J Sci Res Rep 8(5):1–12

Adesina EA, Musa A, Ajayi OG, Odumosu JO, Opaluwa YD, Onuigbo IC (2021) Comparative assessment of SRTM and UAV-Derived dem in flood modelling. Environ Technol Sci J 12(2):58–70. https://doi.org/10.4314/etsj.v12i2.6

Adesina EA, Musa A, Onuigbo IC, Adesiji AR (2022) Assessment of the Hydrological Characteristics of Shiroro Dam, Nigeria. SETIC 2022 International Conference: Sustainable Development and Resilience of the Built Environment in the Era of Pandemic. School of Environmental Technology, Federal University of Technology, Minna. 115–122. ISBN 978-978-54580-8-4

Ahmed B, Zoe L, Wael E (2023) Dam system and reservoir operational safety: A Meta-Research. Water 15(19):3427. https://doi.org/10.3390/w15193427

Ajayi OG (2023) Digital Elevation Models (DEMs). In A. J. Kent & D. Specht (Eds.). The Routledge Handbook of Geospatial Technologies and Society. Routledge Taylor and Francis Inc. Chapter 16, (pp. 226–235). https://doi.org/10.4324/9780367855765

Ajayi OG, Salubi AA, Angbas AF, Odigure MG (2017) Generation of accurate digital elevation models from UAV acquired low percentage overlapping images. Int J Remote Sens 8–10(38):3113–3134. https://doi.org/10.1080/01431161.2017.1285085

Anzaku M, Iliyasu BY, Alfred OF, Idoko AM, Sa'adu SD (2019) Evaluation of environmental effect of Shiroro hydropower dam on the downstream communities of Shiroro local government area, Niger State, Nigeria. J Environ Earth Sci. https://doi.org/10.7176/JEES

Bates DM, De Roo JCD (2000) Mixed-effects modelling of categorical response. J Royal Stat Society: Ser B (Statistical Methodology) 62(1):179–192
Bates PD, Horritt MS, Fewtrell TJ (2010) A simple inertial formulation of the shallow water equations for efficient two-dimensional flood inundation modelling. J Hydrol 387(1–2):33–45
Bijan Fa, Iulii D, Masoud R, Mehdi H, Wiley J (2024) & Sons Ltd on behalf of the Royal Meteorological Society. 1–23. https://doi.org/10.1002/joc.8519
Bounab A, El Kharim Y, El Hamdouni R (2022) The suitability of UAV-Derived DSMs and the impact of DEM resolutions on rockfall numerical simulations: A case study of the Bouanane active scarp, Tétouan, Northern Morocco. Remote sensing. 14:6205. https://doi.org/10.3390/rs14246205
Chai T, Draxler RR (2014) Root mean square error (RMSE) or mean absolute error (MAE)? Arguments against avoiding RMSE in the presence of outliers. Geosci Model Dev 7(3):1247–1250
Chaudhry AQ (2008) Impact of corporate governance regulations on financial markets: evidence from emerging economies. Corp Governance: Int J Bus Soc 8(4):494–506
Chow VT (1959) Open-channel hydraulics. McGraw-Hill
Congalton RG, Green K (2009) Assessing the accuracy of remotely sensed data: principles and practices. CRC press
Cook A, Merwade V (2009) Effect of topographic data, geometric configuration and modelling approach on flood inundation mapping. J Hydrol 377(1):131–142
Coveney S, Fotheringham AS (2011) The impact of DEM data source on prediction of flooding and erosion risk due to sea-level rise. Int J Geogr Inf Sci 25(7):1191–1211
Da Costa RT, Mazzoli P, Bagli S (2019) Limitations posed by free DEMs in watershed studies: the case of river Tanaro in Italy. Frontier Earth Sci 7:141
Dadiyorto W, Bruno M, Norbert M (2019) Assessing hydrograph similarity and rare runoff dynamics by cross recurrence plots. Adv Earth Space Sci. 55:4704–4726. https://doi.org/10.1029/2018WR024111
Dang Y, Chen L, Zhang W, Zheng D, Zhan D (2020) How does growing City size affect residents' happiness in urban China? A case study of the Bohairim area. Habitat Int 97: Article 102120.
Desmond RE, Francis EE, Moses P, Anslem O, Ifunanya O (2024) The impact of dam management and rainfall patterns on flooding in the Niger delta: using Sentinel-1 SAR data. Discover Water 4:123. https://doi.org/10.1007/s43832-024-00185-8
Esmaeel P, Shokoufeh K, Seiyed MH, Yaser JM (2022) Application of unmanned aerial vehicle DEM in flood modelling and comparison with global DEMs: A case study of the Atrak river basin, Iran. J Environ Manage Volume 317:115492. https://doi.org/10.1016/j.jenvman.2022.115492
Fang J, Lincke D, Brown S, Nicholls R, Wolff C, Merkens J, Hinkel J, Vafeidis A (2020) Coastal flood risks in China through the 21st century-An application of DIVA. Sci Total Environ 704: Article 135311.
Farr TG, Rosen PA, Caro E, Crippen R, Duren R, Hensley S, Kobrick M, Paller M, Rodriguez E, Roth L (2007) The shuttle radar topography mission. Rev Geophys 45:1–33
French RH (1985) Open-channel hydraulics. McGraw-Hill
Gafurov A, Kim J (2021) Accuracy assessment of High-Resolution DEMs derived from UAV photogrammetry: A case study in a mountainous area. Remote Sens 13(12):2374
Gaurav A, Erich E, Nathan R, Martin B, Reza S, Drew M, Patrick R (2024) Estimating the influence of water control infrastructure on natural low flow in complex reservoir systems: A case study of the Ohio River. Journal of Hydrology: Regional Studies, Published by Elsevier B.V. This is an open-access article under the CC BY-NC license (http://creativecommons.org/licenses/by-nc/4.0/). https://doi.org/10.1016/j.ejrh.2024.101897
Gu X, Wang L, Liu Y, Zhang W, Zhang Y (2019) A review of digital elevation models (DEMs) for terrain analysis and hydrological modeling. J Mt Sci 16(11):2585–2606
Hannes N, Milad A, Kaveh M, Nima S (2024) Quantifying water evaporation from large reservoirs: Implications for water management in water-stressed regions. Environ Res 262, Part 1, 119860. https://doi.org/10.1016/j.envres.2024.119860
Hengkang Z, Yangbo C (2024) A study of the effect of DEM Spatial resolution on flood simulation in distributed hydrological modelling. Remote Sens 16(16):3105. https://doi.org/10.3390/rs16163105
Horritt NK, Bates PD (2002) Evaluation of 1D and 2D numerical models for predicting river flood inundation. J Hydrol 268(1–4):87–99
Jayanthi SLV, Keesara VR, Sridhar V (2022) Prediction of future lake water availability using SWAT and support vector regression (SVR). Sustainability 14(12):6974. https://doi.org/10.3390/su14126974
Kemp D, Daniell T (2020) A review of flow Estimation by runoff routing in Australia–and the way forward. J Water Resource 24:139–152. https://doi.org/10.1080/13241583.2020.1810927
Kim Y, Tak Y, Park M, Kang B (2020) Improvement of urban flood damage Estimation using a high-resolution digital terrain. J Flood Risk Manag 13(S1): Article e12575.
Kim D, Han H, Lee H, Kang Y, Wang W, Kim HS (2024) Predicting flood water level using a combined hybrid model of rainfall-runoff and AI-Based models. KSCE J Civ Eng 28:1580–1593

Lane SN, Brookes CJ, Kirkby MJ, Holden J (1998) A grid-based simulation model of river flood inundation. Hydrol Process 12(8):1331–1351

Legates DR, McCabe GJ Jr (1999) Evaluating the use of goodness-of-fit measures in hydrologic and hydroclimatic model validation. Water Resour Res 35(1):233–241

Leitao JP, Moy De Vitry M, Scheidegger A, Rieckermann J (2016) Assessing the quality of digital elevation models obtained from mini unmanned aerial vehicles for overland flow modelling in urban areas. Hydrol Earth Syst Sci 20(4):1637–1653. https://doi.org/10.5194/hess-20-1637-2016

Lurton X (2010) Sonar performance. Springer Science & Business Media

Maidment DR (ed) (2002) Handbook of hydrology. McGraw-Hill

Massazza G, Tamagnone P, Wilcox C, Belcore E, Pezzoli A, Vischel T, Panthou G, Ibrahim MH, Tiepolo M, Tarchiani V (2019) Flood hazard scenarios of the Sirba river (Niger): evaluation of the hazard thresholds and flooding areas. Water 11:1018

Merwade V, Olivera F, Arabi M, Edelen A (2008) GIS-based flood inundation mapping. Comput Geosci 34(10):1175–1183

Mohamed M, Brijesh KY, Mwemezi JR, Isaac L, Sam-Quarcoo D, Andrew ML, Solomon S, Daniel K (2022) Rainfall and temperature changes under different climate scenarios at the watersheds surrounding the Ngorongoro conservation area in Tanzania. Environ Chall. 7:100446. https://doi.org/10.1016/j.envc.2022.100446

Moustakis Y, Papalexiou SM, Onof CJ, Paschalis A (2021) Seasonality, intensity, and duration of rainfall extremes change in a warmer climate. Earth's Future 9:1–15. https://doi.org/10.1029/2020EF001824

Mukherjee S, Joshi PK, Mukherjee S, Ghosh A, Garg RD, Mukhopadhyay A (2013) Evaluation of vertical accuracy of open source digital elevation model (DEM). Int J Appl Earth Obs Geoinf 21(1):205–217

Muyuan X, Lelys B, José RC (2023) Climate change impacts on rainfall intensity–duration–frequency curves in local scale catchments. Environ Monit 196:372. https://doi.org/10.1007/s10661-024-12532-2

Nageswara Rao K, Raju KVS, Kumar B (2022) Distributed hydrological modeling using SWAT for assessing the impact of land use and climate change on water resources in a semi-arid region. J Water Clim Change 13(1):223–242

Niger State Emergency Management Agency (NSEMA) (2022) Studies Conducted to Determine Flood Risk Communities Affected by Violent Water within Niger State, Nigeria

Nigerian Emergency Management Agency (NEMA) (2024) Floods– Situation Report

O'Connell PE, Beven KJ, Young PC (2010) Rainfall–runoff modelling: the challenge of complexity. Hydrol Res 41(3–4):219–246

Okeke FI (2006) InSAR Operational and Processing Steps for DEM Generation. Promoting Land Administration and Good Governance. 5th FIG Regional Conference Accra, Ghana. 1–13

Özdemir H, Akbaş B (2015) Comparison of DEM generation methods using GPS, total station, and UAV data in a mountainous area. Measurement 73:490–498

Pappenberger F, Beven KJ, Horritt N, Bath A (2007) Uncertainty assessment of flood inundation predictions using fuzzy number representation. J Hydrol 342(3–4):291–307

Pedrozo-Acuna A, Rodrıguez-Rincon J, Arganis-Juarez M, Domınguez-Mora R, Gonzalez VF (2015) Estimation of probabilistic flood inundation maps for an extreme event: Pa´nuco river, Mexico. J Flood Risk Manag 8(2):177–192

Rosen PA, Hensley S, Joughin IR, Li YS, Madsen SN, Rodriguez E, Goldstein RM (2000) Synthetic aperture radar interferometry. Proceedings of the IEEE 88(3), 333–382

Sahu MK, Shwetha HR, Dwarakish GS (2023) State-of-the-art hydrological models and application of the HEC-HMS model: a review. Model Earth Syst Environ. https://doi.org/10.1007/s40808-023-01704-7

Saksena S, Merwade V (2015) Incorporating the effect of DEM resolution and accuracy for improved flood inundation mapping. J Hydrol 530:180–194

Sanaz M, Ammar S, Mohammad A (2023) Performance of the flood models in different topographies. J Hydrol 620(2):129446. https://doi.org/10.1016/j.jhydrol.2023.129446

Savage J, Pianosi F, Bates P, Freer J, Wagener T (2016) Quantifying the importance of Spatial resolution and other factors through global sensitivity analysis of a flood inundation model. Water Resour Res 52(11):9146–9163

Schumann GJP, Bates PD (2020) Editorial: the need for a High-Accuracy. Open-Access Global Digit Elevation Model Frontier Earth Sci 8:618194

Shiroro Dam Authority (2020) Hydrological Data, 2020. Data provided by the Shiroro Dam Authority, Shiroro

Simpson MJ, Bates PD, Tiggelovend JJ, Wilson MD, De Roo APJ (2016) Large-scale flood inundation mapping: a comparison of methodologies. Hydrol Process 30(1):148–161

Skidmore AK (1989) A spatially-accurate technique for the creation of land use maps from remotely sensed data. Int J Remote Sens 10(7):1199–1216

Slater JA, Garvey G, Johnston C, Haase J, Heady B, Kroenung G, Little J (2006) The SRTM data 'finishing' process and products, photogrammetry. Eng Remote Sens 72:237–247

Niger State Geographic Information System (NIGIS) (2022) Settlement data for the study area. Retrieved 2022, from https://nigisservices.com/

Spina V, Amoyedo S, Wibberley C, Tozer R, Ribes C, Maia R, Atoyebi H, Vincent E (2025) Characterization of a deep-water turbiditic reservoir under an active hydrodynamic regime (Niger Delta). Mar Petr Geol. 172:107185. https://doi.org/10.1016/j.marpetgeo.2024.107185

Sridhar V, Kang H, Ali SA (2019) Human-induced alterations to land use and climate and their responses on hydrology and water management in the Mekong river basin. Water 11:1307. https://doi.org/10.3390/w11061307

Sridhar V, Ali SA, Sample DJ (2021) Systems analysis of coupled natural and human processes in the Mekong river basin. Hydrology 8:140. https://doi.org/10.3390/hydrology8030140

Suleiman YM (2014) The role of rainfall variability in reservoir storage management at Shiroro hydropower dam, Nigeria. Int J Sci Technol 3(2):2. https://doi.org/10.4314/stech.v3i2

Syahida FA, Lariyah MS, Kahhoong K, Sarbani AA, Darul HS, Siti MA, Hidayah B, Mohd HZ, Ali NA (2023) Assessing dam spillway discharge capacity in response to extreme floods in Perak river hydroelectric scheme: simulation and proposed mitigation measures. Ain Shams Eng J Volume 14(11):102540. https://doi.org/10.1016/j.asej.2023.102540

Syed AA, Noor MK, Muhammad KS, Muhammad WZ, Atiq UT, Ubaid U, Yasir A (2024) Hydraulic investigation of flows at high-head overflow spillway with multiple aerators: a physical and numerical study of Mohmand dam, Pakistan. AQUA-Water Infrastructure Ecosyst Soc 73:1725. https://doi.org/10.2166/aqua.2024.180

Talchabhadel R, Nakagawa H, Kawaike K, Yamanoi K, Thapa BR (2021) Assessment of vertical accuracy of open source 30m resolution space-borne digital elevation models. Geomatics Nat Hazards Risk 12(1):939–960

Tarboton DG (1997) A new method for determining flow directions and upslope areas in grid digital elevation models. Water Resour Res 33(3):309–319

Toro EF (2001) Shock-capturing methods for free-surface shallow flows. John Wiley & Sons

Usman A, Ifabiyi I (2012) Socio-Economic analysis of the operational impacts of Shiroro hydropower generation in the lowland. Int J Acad Res Bus Social Sci 2(4):2222–6990

Utlu Ö, Özdemir H (2020) Comparison of DEM generation methods from UAV photogrammetry and lidar data. Eur J Remote Sens 53(1):162–176

Vinh NT, Jongho K (2024) UIDS: A Matlab-based urban flood model considering rainfall-induced and surcharge-induced inundations. Environ Modelling Softw Volume 179:106132. https://doi.org/10.1016/j.envsoft.2024.106132

Werner MGF, Hunter NM, Bates PD (2005) Identifiability of distributed floodplain roughness parameters in GIS-based flood inundation models. J Hydrol 314(1–4):136–157

Wilson JP, Gallant JC (eds) (2000) Terrain analysis: principles and applications. John Wiley & Sons

Xingyu Z, Lunwu M, Tianqi A, Xiaorong H, Haiyan Y (2024) Effect of Spatial Resolution of Digital Terrain by Drone on Mountainous Urban Fluvial Flood Modelling. Egusphere Preprint Repository. https://doi.org/10.5194/egusphere-2024-404

Xuefei M, Van Gelder PHAJM, Zhijun D, Zhenghong T Impact of dams on flood occurrence of selected rivers in the United States. Higher Education, Press (2016) and Springer-Verlag Berlin Heidelberg. Frontiers of Earth Science 11(2). https://doi.org/10.1007/s11707-016-0592-1

Yaru Z, Haijun Q, Zijing L, Bingfeng Ye, Bingzhe T, Yijun L, Ulrich K (2024) Rainfall and water level fluctuations dominated the landslide deformation at Baihetan reservoir, China. J Hydrology Volume 642:131871. https://doi.org/10.1016/j.jhydrol.2024.131871

Yousra M, Khir A, Lee L (2021) Impacts of dams on the environment: A review. Int J Environ Agric Biotechnol 6(1):064–074. https://doi.org/10.22161/ijeab.61.9

Yudai E, Sou N, Yusuke S, Haruhiko N, Takashi K, Nina S, Kazuyuki A (2024) Impact of time-history terms on reservoir dynamics and prediction accuracy in echo state networks. Sci Rep 14:8631. https://doi.org/10.1038/s41598-024-59143-y

Zhang KD, Gann M, Ross Q, Robertson J, Sarmiento S, Santana J, Rhome C (2019) Accuracy assessment of ASTER, SRTM, ALOS, and TDX DEMs for Hispaniola and implications for mapping vulnerability to coastal flooding. Remote Sens Environ 225:290–306

http://earthexplorer.usgs.gov

https://scihub.copernicus.eu/dhus/#/home.